Catastrophic Collapse of Ultrashort Pulses

Alexander L. Gaeta
School of Applied and Engineering Physics, Cornell University, Ithaca, New York 14853
(Received 28 October 1999)

We investigate theoretically the self-focusing dynamics of an ultrashort laser pulse both near and above the threshold at which the pulse effectively undergoes catastrophic collapse. We find that, as a result of space-time focusing and self-steepening, an "optical shock" wave forms inside the medium that gives rise to a broad blueshifted pedestal in the transmitted pulse spectrum. Our results are in good agreement with the primary features observed in experiments and thus provide a theoretical understanding for the underlying process that gives rise to "white-light" generation.

PACS numbers: 42.65.Jx, 42.25.Bs, 42.65.Re

The nonlinear propagation of an ultrashort pulse through a transparent medium can result in dramatic changes to its temporal, spatial, and spectral properties. The primary process responsible for these changes is self-focusing which causes the pulse to be compressed in space, resulting in a corresponding increase in the peak intensity. For input powers that are above the critical power P_{cr} for self-focusing, steady-state theoretical analysis predicts that the pulse will undergo catastrophic collapse [1]. Similar forms of wave collapse appear in many areas of physics [2]. For experiments in the long-pulse (>1 ns) regime this behavior results in the formation of a plasma which can lead to filamentation [3] and damage [4]. For femtosecond pulses, theoretical and experimental work has shown that the effects of dispersion in the medium completely alter the dynamics of the self-focusing process. For example, even for input powers significantly above the critical power for self-focusing, the effects of dispersion can halt the explosive increase in the peak intensity through the process of pulse splitting [5–7]. More recent theoretical and experimental results [8–11] indicate that, for input pulses significantly longer than a single optical cycle, it is necessary to apply a theoretical model that goes beyond the slowly varying envelope equation in time in order to capture properly the pulse-splitting dynamics.

At sufficiently high input powers, self-focusing still overcomes dispersive effects, leading to an explosive increase in the peak intensity and to the occurrence of other higher-order nonlinear optical processes. Experimentally it is found that, as the input power is increased above a certain threshold power $P_{\mathrm{th}} > P_{\mathrm{cr}}$, an extremely broad pedestal appears on the blue side of the transmitted pulse spectrum. This process is termed supercontinuum generation (SCG) or "white-light" generation [12]. This phenomenon was first observed [13] in 1970, and since then it has been observed in many different solids [14–16], liquids [17], and gases [18] under a wide variety of experimental conditions. The shapes of the observed spectra for various media are similar which suggests that supercontinuum generation is a universal feature of the laser-matter interaction. For spectroscopic applications [12], SCG has proven to be a useful source of broadly tunable ultrafast pulses from the near ultraviolet to the far infrared. Recent work [15,16] in solids shows that the cutoff wavelength on the blue side scales roughly with the band gap of the material and that, as long as the ratio of the band-gap energy to the photon energy is equal to or greater than four, SCG can occur. Despite these numerous studies, the basic underlying process responsible for SCG has resisted explanation via any of the standard nonlinear optical mechanisms. For example, one-dimensional models [19] that incorporate self-phase modulation and self-steepening predict spectra that are qualitatively inconsistent with the observed spectra.

In this Letter, we present a theoretical model that allows us to investigate the dynamics of self-focusing of femtosecond laser pulses both near and above the point at which the pulse effectively undergoes catastrophic collapse. We show that, as the pulse approaches the collapse point, a steep edge is formed at the back of the pulse (i.e., an optical "shock wave") and is accompanied by a large phase jump. The resulting pulse spectrum exhibits a broad blueshifted pedestal with a sharp cutoff, which is in good qualitative agreement with the experimentally observed SCG spectrum. These results show that shock formation due to space-time focusing and self-steepening dictate the collapse dynamics and that the role of multiphoton absorption and plasma formation is simply to halt the collapse at the powers significantly above the threshold for collapse. Our results thus provide the first theoretical basis for a description of the underlying mechanisms for SCG.

We model pulse propagation above the regime of critical collapse by modifying the nonlinear envelope equation (NEE) [20] to include the effects of multiphoton absorption (MPA) and plasma formation. We assume that the pulse has radial symmetry and that it propagates along the z axis with a wave vector amplitude $k = n_0\omega/c$, where n_0 is the linear refractive index of the material and ω is the central frequency of the pulse. We take the input pulse at $z = 0$ to be Gaussian in space and time, such that $A(r, z = 0, t) = A_0 \exp[-r^2/2w_0^2 - t^2/2\tau_p^2]$. In this case, the equation for

 0031-9007/00/84(16)/3582(4)$15.00

the normalized amplitude $u(r,z,t) = A(r,z,t)/A_0$ can be expressed as

$$\frac{\partial u}{\partial \zeta} = \frac{i}{4}\left(1 + \frac{i}{\omega\tau_p}\frac{\partial}{\partial\tau}\right)^{-1}\nabla_\perp^2 u - i\frac{L_{\rm df}}{L_{\rm ds}}\frac{\partial^2 u}{\partial\tau^2} + i\left(1 + \frac{i}{\omega\tau_p}\frac{\partial}{\partial\tau}\right)p_{\rm nl}, \quad (1)$$

where $L_{\rm df} = kw_0^2/2$ is the diffraction length, $\zeta = z/L_{\rm df}$ is the normalized distance, $L_{\rm ds} = \tau_p^2/\beta_2$ is the dispersion length, β_2 is the group-velocity dispersion, $\tau = (t - z/v_g)/\tau_p$ is the normalized retarded time for the pulse traveling at the group velocity v_g, and $p_{\rm nl}$ is the suitably normalized nonlinear polarization. The presence of the operator $(1 + i\partial/\omega\tau_p\partial\tau)$ in the diffraction and the nonlinear polarization terms gives rise to space-time focusing [8] and self-steepening effects [19], respectively, and allows for the modeling of pulses with spectral widths comparable to the optical frequency ω. In the expression for the nonlinear polarization we include the effects of the nonlinear refractive index change, multiphoton absorption, and formation of an electron plasma density ρ_e such that

$$p_{\rm nl} = \frac{L_{\rm df}}{L_{\rm nl}}|u|^2 u - \frac{L_{\rm df}}{L_{\rm pl}}(1 - i/\omega\tau_c)\rho u + i\frac{L_{\rm df}}{L_{\rm mp}}|u|^{2(m-1)}u, \quad (2)$$

where $L_{\rm nl} = (c/\omega n_2 I_0)$ is the nonlinear length, $I_0 = n_0 c|A_0|^2/2\pi$ is the peak input intensity, τ_c is the electron collision time, $L_{\rm mp} = 1/\beta^{(m)}I_0^{(m-1)}$ is the m-photon absorption length, $\beta^{(m)}$ is the m-photon absorption coefficient, $L_{\rm pl} = 2\rho_0/\sigma\omega\tau_c$ is the plasma length, σ is the cross section for inverse bremsstrahlung, and $\rho = \rho_e/\rho_0$ is the electron density normalized to the total density $\rho_0 = \beta^{(m)}I_0^m\tau_p/n\hbar\omega$ of electrons that would be produced by the input pulse through multiphoton absorption. We assume that the electron density can grow in the presence of the laser field through avalanche ionization and multiphoton absorption, such that ρ satisfies the equation

$$\frac{\partial\rho}{\partial\tau} = \alpha\rho|u|^2 + |u|^{2m}, \quad (3)$$

where $\alpha = \sigma I_0\tau_p/n_0^2 E_g$ is the avalanche ionization coefficient and E_g is the band-gap energy of the material. A similar form of the nonlinear polarization has been used to model self-focusing in water [21] and in air [22]; however, in these studies space-time focusing and self-steepening terms were not included. We have also performed simulations with the inclusion of noninstantaneous contribution to the nonlinear refractive index (i.e., stimulated Raman scattering); however, the presence of this term does not alter substantially the behavior presented here, and, for certain materials such as sapphire [23] and the alkali halides, this term can be neglected. From simulations of steady-state self-focusing with only the nonlinear refractive index term [24], the relationship of the ratio $L_{\rm df}/L_{\rm nl}$ to the ratio $P/P_{\rm cr}$ is given by $L_{\rm df}/L_{\rm nl} = 0.948P/P_{\rm cr}$.

In our simulations we use parameters that correspond to the case of a 5-mm-thick sapphire sample and a 70 fs input pulse at a wavelength of 800 nm. For sapphire, $\beta_2 = 1280\ \mathrm{fs^2/cm}$ and $n_2 = 3 \times 10^{-16}\ \mathrm{cm^2/W}$ which corresponds to $L_{\rm ds} = 1.4$ cm and $P_{\rm cr} = 1.8$ MW. The value of $\omega\tau_p = 100$, and we assume that the beam is focused loosely into the sample such as that in the $L_{\rm df}/L_{\rm ds} = 0.15$. Ultimately, the qualitative behavior of the system we describe here occurs over a wide range of input parameters and thus does not depend sensitively on the specific values.

We first consider the case in which we do not include multiphoton absorption or plasma formation in our model. We find in our simulations that, as the input power is increased to a certain threshold power $P_{\rm th}$, which is determined by the ratio of $L_{\rm df}/L_{\rm ds}$ [25], the peak intensity grows sharply. This is illustrated in Fig. 1, where we plot the peak intensity as a function of distance in the medium for $P/P_{\rm cr} = 1.7$ and 1.8. In both cases dispersion and temporal pulse splitting halt the collapse of the pulse. In Fig. 2(a) we plot the on-axis temporal profile and frequency chirp (i.e., $-\partial\phi/\partial\tau$, where ϕ is the phase) for $P/P_{\rm cr} = 1.7$ at $\zeta = 2$ which is past the point of maximum peak intensity and just at the onset of pulse splitting. Space-time focusing and self-steepening act to push the peak intensity towards the rear of the pulse, and the frequency chirp exhibits a dispersive-looking shape with a blueshift (redshift) at the back (front) of the pulse. The total spectrum for this pulse is asymmetric [dotted line in Fig. 2(d)] with a pronounced blue tail. Figures 2(b) and 2(c) show the on-axis temporal profile and frequency chirp at two different points in the medium at slightly higher power $P/P_{\rm cr} = 1.8$. At $\zeta = 1.63$ the blueshifted feature in the chirp becomes narrower and is more pronounced, and the spectrum [dashed line in Fig. 2(d)] shows increased asymmetry. At the point ($\zeta = 1.7$) near where

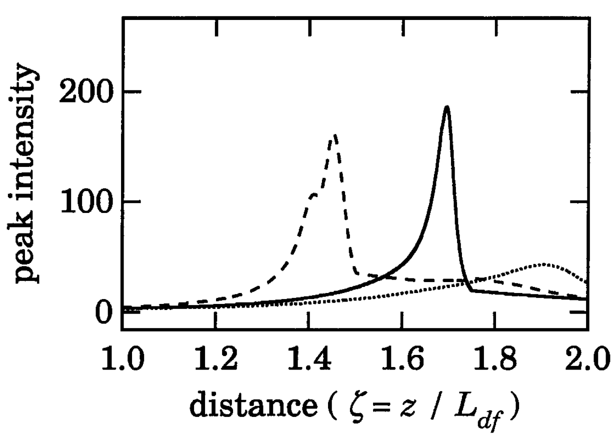

FIG. 1. Plot of normalized peak intensity inside the medium as a function of distance $\zeta = z/L_{\rm df}$ for $P/P_{\rm cr} = 1.7$ (dotted line) and $P/P_{\rm cr} = 1.8$ (solid line) in the absence of multiphoton absorption (MPA) and plasma formation, and for $P/P_{\rm cr} = 2$ (dashed line) with the inclusion of MPA and plasma formation.

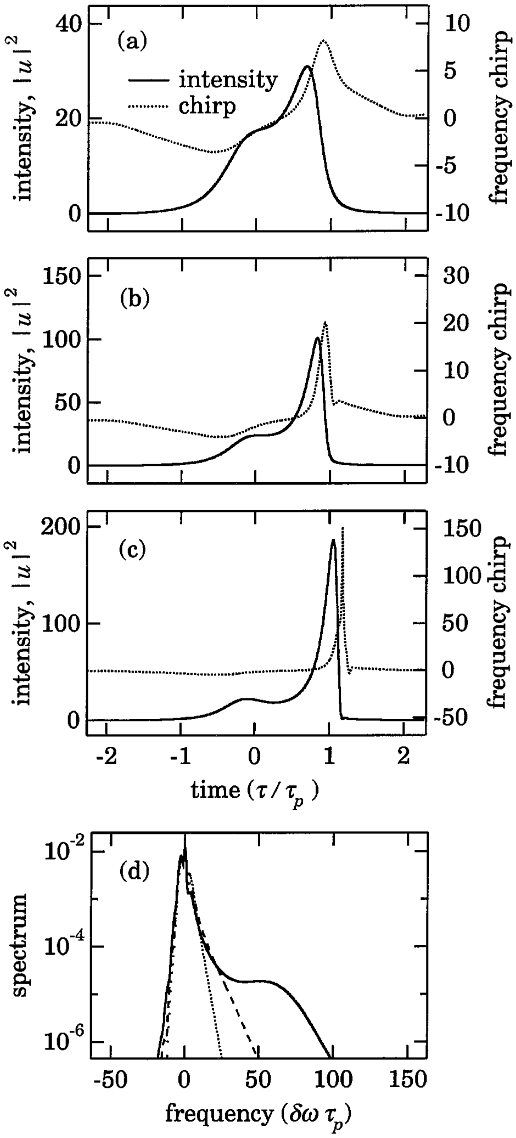

FIG. 2. On-axis temporal intensity profile and frequency chirp [(a)–(c)] and the corresponding total pulse spectra (d) in the absence of multiphoton absorption and plasma formation. In (a) $P/P_{\rm cr} = 1.7$ and $\zeta = z/L_{\rm df} = 2$. In (b) and (c) $\zeta = 1.63$ and $\zeta = 1.7$, respectively, and $P/P_{\rm cr} = 1.8$.

the intensity peaks, the steepness at the back edge of the pulse is maximized, and the frequency chirp forms a narrow peak at the back edge [Fig. 2(c)]. It is at this point that the phase of the pulse undergoes an abrupt decrease in a time comparable to the optical period and the formation of a long blue pedestal in the pulse spectrum with a sharp cutoff [solid line in Fig. 2(d)]. For larger distances into the medium the pulse spectrum stabilizes and shows little change from that shown in Fig. 2(d). This spectrum shows strong qualitative agreement with supercontinuum spectra observed near threshold in solids [15,16].

In our simulations, we find that the width of the pedestal is determined by the magnitude of the induced frequency chirp, which in turn is determined by the peak intensity of the shock wave. Slight increases in the input power beyond $P/P_{\rm cr} = 1.8$ lead to explosive growth in the peak intensity and in the steepness of the back edge of the pulse, making numerical computation difficult. It is still an open question whether for sufficiently high intensity the NEE does in fact possess a singularity in the absence of MPA and plasma formation. However, from a practical perspective the pulse can be viewed as having undergone catastrophic collapse, since in any real experiment the peak intensity exhibits explosive growth and contributions from MPA and plasma formation must be taken into account. The inclusion of these processes halts the explosive growth in intensity and allows for simulations substantially above the $P_{\rm th}$.

Figure 1 shows a plot of the peak intensity inside the medium for $P/P_{\rm cr} = 2$ where MPA, plasma formation, and plasma defocusing prevent collapse of the pulse. The parameters for the MPA and plasma terms are assumed to be that of sapphire, in which case $m = 5$, $\omega\tau_c = 5$, and $L_{\rm df}/L_{\rm pl} = 10^{-9}$. Ultimately, the qualitative behavior of the system does not depend sensitively on these values, and the resulting evolution of the pulse is found to be similar to the case of $P/P_{\rm cr} = 1.8$ in which the collapse was halted only by dispersion. Figure 3(a) shows the temporal profile and frequency chirp at the point in the medium $\zeta = 1.53$, where the abrupt phase jump occurs, and Fig. 3(c) shows the corresponding total pulse spectrum. As in the previous case, the spectrum develops a broad pedestal on the blue side with minimal broadening towards the red side. We find that further increases in the input pulse power do not lead to increased broadening of the pedestal but do result in broadening towards the red side, which is also consistent with experimental observations.

Although it has been proposed [15,26] that plasma formation may be responsible for the blueshifted pedestal in SCG, we find for the self-focusing interaction that actually the opposite is true. If the space-time focusing and self-steepening terms are neglected, we find that the presence of the plasma terms pushes the peak intensity to the front edge of the pulse since the plasma formation results in defocusing and nonlinear absorption of the back edge. As a result, the pulse develops a steep edge at the front [see Fig. 3(b)] and a corresponding abrupt increase in the phase which produces a negative frequency chirp. As a result, a redshifted pedestal appears in the generated spectrum [see Fig. 3(c)].

We find that the temporal and spectral behavior that produces SCG occurs over a wide range of parameters as long as the input focusing conditions of the beam are such that shock formation can occur before MPA and plasma formation dominate the interaction. For example, we find that, for similar conditions but smaller values of m (e.g., $m \leq 3$), the collapse is halted before significant pulse steepening occurs which prevents the occurrence of a phase jump and SCG. In addition, if the initial focusing conditions are such that the beam is tightly focused into the material such that the linear focusing is responsible for creating sufficiently high intensities to create a plasma, then

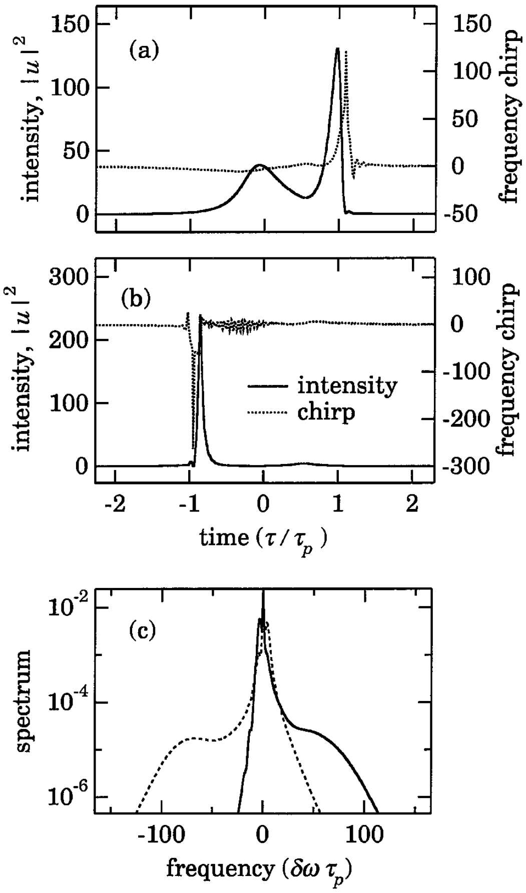

FIG. 3. (a) On-axis temporal intensity profile and frequency chirp with the inclusion of multiphoton absorption and plasma formation for the same parameters as in Fig. 2 but with $P/P_{\mathrm{cr}} = 2$ and $\zeta = z/L_{\mathrm{df}} = 1.46$. The corresponding total pulse spectrum is given by the solid line in (c). (b) Same as in (a), but at $\zeta = 1.53$ and without the space-time focusing and self-steepening contributions. The corresponding total pulse spectrum is given by the dashed line in (c).

SCG is also not observed. These results agree with our own experimental observations [27] and that of others [15,16].

In all of the cases we have studied, we find for pulses in the femtosecond regime that, although MPA provides the initial density of free electrons, avalanche ionization dominates the total production of the plasma density. Nevertheless, even for powers that are several times above P_{th}, the peak plasma density remains significantly below the critical plasma density of $\sim 2 \times 10^{21}$ cm^{-3} inside the medium. These results suggest that, unlike the long-pulse regime (e.g., nanosecond pulses), the temporal dynamics of self-focusing collapse with the femtosecond pulses is such that catastrophic damage to the material is not predicted to occur.

In conclusion, we have investigated the nonlinear dynamics of ultrashort pulse propagation both near and above the threshold for self-focusing collapse, and we find that our results our in good agreement with experimental observations. We show that the formation of an optical shock wave at the back of the pulse is the likely explanation for the process of supercontinuum generation. These results are also relevant to bulk damage in solid-state materials and to propagation experiments in gases including filamentation in air.

We gratefully acknowledge illuminating discussions with A. Brodeur, N. Bloembergen, C. Shaffer, E. Mazur, K. Moll, J. Ranka, and A. Streltsov. This work was supported by the National Science Foundation.

[1] See, for example, Y. S. Kivshar and D. E. Pelinovsky, Rev. Mod. Phys. (to be published).
[2] See, for example, P. A. Robinson, Rev. Mod. Phys. **69**, 507 (1997).
[3] R. Y. Chiao *et al.*, Phys. Rev. Lett. **13**, 479 (1964); Y. R. Shen and M. T. Loy, Phys. Rev. A **3**, 2099 (1971); E. Yablonovitch and N. Bloembergen, Phys. Rev. Lett. **29**, 907 (1972).
[4] N. Bloembergen, IEEE J. Quantum Electron. **QE-19**, 375 (1974).
[5] N. Zharova *et al.*, Pis'ma Zh. Eksp. Teor. Fiz. **44**, 12 (1986) [JETP Lett. **44**, 13 (1986)]; J. E. Rothenberg, Opt. Lett. **17**, 583 (1992); P. Chernev and V. Petrov, Opt. Lett. **17**, 172 (1992); G. G. Luther *et al.*, Opt. Lett. **19**, 789 (1994); G. Fibich, V. M. Malkin, and G. C. Papanicolaou, Phys. Rev. A **52**, 4218 (1995); L. Bergé *et al.*, J. Opt. Soc. Am. B **20**, 1879 (1996).
[6] J. K. Ranka *et al.*, Phys. Rev. Lett. **77**, 3783 (1996).
[7] S. A. Diddams *et al.*, Opt. Lett. **23**, 379 (1998).
[8] J. E. Rothenberg, Opt. Lett. **17**, 1340 (1992).
[9] G. Fibich and G. C. Papanicolaou, Opt. Lett. **22**, 1379 (1997).
[10] J. K. Ranka and A. L. Gaeta, Opt. Lett. **23**, 534 (1998).
[11] A. A. Zozulya *et al.*, Phys. Rev. Lett. **82**, 1430 (1999); A. A. Zozulya *et al.*, Phys. Rev. A **58**, 3303 (1998).
[12] See, for example, *The Supercontinuum Laser Source*, edited by R. R. Alfano (Springer-Verlag, New York, 1989).
[13] R. R. Alfano and S. L. Shapiro, Phys. Rev. Lett. **24**, 584 (1970); **24**, 592 (1970).
[14] P. B. Corkum *et al.*, Opt. Lett. **10**, 624 (1985).
[15] A. Brodeur and S. L. Chin, Phys. Rev. Lett. **80**, 4406 (1998); A. Brodeur and S. L. Chin, J. Opt. Soc. Am. B **16**, 637 (1999).
[16] A. Brodeur *et al.* (to be published).
[17] W. L. Smith *et al.*, Phys. Rev. A **15**, 2396 (1977); R. L. Fork *et al.*, Opt. Lett. **8**, 1 (1983).
[18] P. B. Corkum *et al.*, Phys. Rev. Lett. **57**, 2268 (1986); J. H. Glownia *et al.*, J. Opt. Soc. Am. B **3**, 1573 (1986); V. Francois *et al.*, Opt. Commun. **99**, 241 (1993).
[19] G. Yang and Y. R. Shen, Opt. Lett. **9**, 510 (1984).
[20] T. Brabec and F. Krausz, Phys. Rev. Lett. **78**, 3282 (1997).
[21] Q. Feng *et al.*, IEEE J. Quantum Electron. **QE-33**, 127 (1997).
[22] M. Mlejnek *et al.*, Opt. Lett. **23**, 382 (1998).
[23] S. Smolorz and F. W. Wise (unpublished).
[24] G. Fibich and A. L. Gaeta, Opt. Lett. **25**, 335 (2000).
[25] G. G. Luther *et al.*, Opt. Lett. **19**, 862 (1994); C. Cerullo *et al.*, Opt. Lett. **21**, 65 (1996).
[26] N. Bloembergen, Opt. Commun. **73**, 285 (1973).
[27] K. D. Moll, A. M. Streltsov, and A. L. Gaeta (unpublished).